

Pelvic schwannoma misdiagnosed as colorectal cancer metastasis and the corresponding diagnostic lessons: A report of two cases

SHILONG WANG^{1,2}, KAIXIANG ZHANG^{2,3}, XIANGWU LIN^{2,3}, FEILAI XIE^{3,4}, JIAN YANG^{3,5} and JIE LI¹⁻³

¹Department of Oncology, Fuzong Teaching Hospital of Fujian University of Traditional Chinese Medicine (900th Hospital), Fuzhou, Fujian 350025, P.R. China; ²Department of Oncology, 900th Hospital of PLA Joint Logistic Support Force, Fuzhou, Fujian 350025, P.R. China; ³Fuzong Clinical Medical College of Fujian Medical University, Fuzhou, Fujian 350025, P.R. China; ⁴Department of Pathology, 900th Hospital of PLA Joint Logistic Support Force, Fuzhou, Fujian 350025, P.R. China; ⁵Department of Radiology, 900th Hospital of PLA Joint Logistic Support Force, Fuzhou, Fujian 350025, P.R. China

Received December 16, 2025; Accepted April 13, 2026

DOI: 10.3892/ol.2026.15659

Abstract. Schwannomas are neurogenic tumours originating from Schwann cells, and the vast majority of the tumours are benign lesions. Schwannomas are most commonly found in the head, neck and extremities; however, those occurring in the pelvis are rare. Due to the lack of specific clinical manifestations and radiographic features, pelvic schwannomas are difficult to detect and differentiate at an early stage. Cases of pelvic schwannomas coexisting with colorectal cancer have rarely been reported in both domestic and international literature. The current study presents two cases of pelvic schwannomas that were misdiagnosed as colorectal cancer metastases. Both lesions were initially identified as metastatic colorectal cancer during preoperative evaluation and were subsequently confirmed as schwannomas by postoperative pathological examination. This report analyses the causes of misdiagnosis, summarises the key distinguishing features between pelvic schwannomas and colorectal cancer metastases, and proposes a diagnostic algorithm for patients with colorectal cancer and pelvic masses of uncertain origin, with the aim of providing practical guidance for clinical practice.

Introduction

It is generally accepted that schwannomas are neurogenic tumours originating from Schwann cells (1). Schwannomas demonstrate a predilection for the head, neck and extremities, and those originating in the pelvis are rare, accounting for only 1-3% of all schwannomas according to the relevant

literature (2). In most cases, schwannomas are benign lesions that typically do not require adjuvant therapy following surgery and are associated with a low recurrence rate (3-5). However, pelvic schwannomas are challenging to detect and difficult to identify at an early stage due to the lack of specific clinical manifestations and imaging features (6,7). A definitive diagnosis requires histopathological confirmation, characterized by the typical alternating hypercellular Antoni A areas and hypocellular Antoni B areas composed of spindle cells, along with strong and diffuse S-100 protein immunohistochemical positivity (8). At present, reports of pelvic schwannomas concomitant with colorectal cancer are limited. In the two cases reported in the present study, colorectal cancer was the primary diagnosis in both patients, and the lesions were initially considered pelvic metastases preoperatively, with schwannomas subsequently confirmed by postoperative pathological examination. Misdiagnosis may lead to inaccurate tumour staging and may result in missed opportunities for radical surgery. The present report retrospectively analyses these cases, summarises the findings, and proposes relevant strategies to improve future clinical diagnosis.

Case report

Case 1. A 55-year-old female patient presented to the 900th Hospital of PLA Joint Logistic Support Force (Fuzhou, China) with a 3-day history of constipation and a 1-day history of lower abdominal pain and discomfort. Colonoscopy revealed a circumferential mass located 17 cm from the anal verge, with luminal obstruction preventing passage of the endoscope. Biopsy pathology indicated high-grade atypical hyperplasia of the adenomatous epithelium/intraepithelial neoplasia and carcinoma (Fig. S1A) [all biopsy and surgical specimens were fixed in 10% neutral buffered formalin at room temperature for 24-48 h, routinely dehydrated and embedded in paraffin. Serial sections (3- μ m thick) were prepared, and hematoxylin and eosin staining was performed at 28°C for 15 min. Slides were examined using an OLYMPUS BX53 light microscope (Olympus Corporation), with magnifications indicated in the respective figure legends]. Whole-body 18F-fluorodeoxyglucose

Correspondence to: Professor Jie Li, Department of Oncology, 900th Hospital of PLA Joint Logistic Support Force, 156 West Second Ring Road North, Gulou, Fuzhou, Fujian 350025, P.R. China
E-mail: 13960756219@139.com

Key words: schwannoma, pelvic cavity, colorectal cancer, misdiagnosis, differential diagnosis

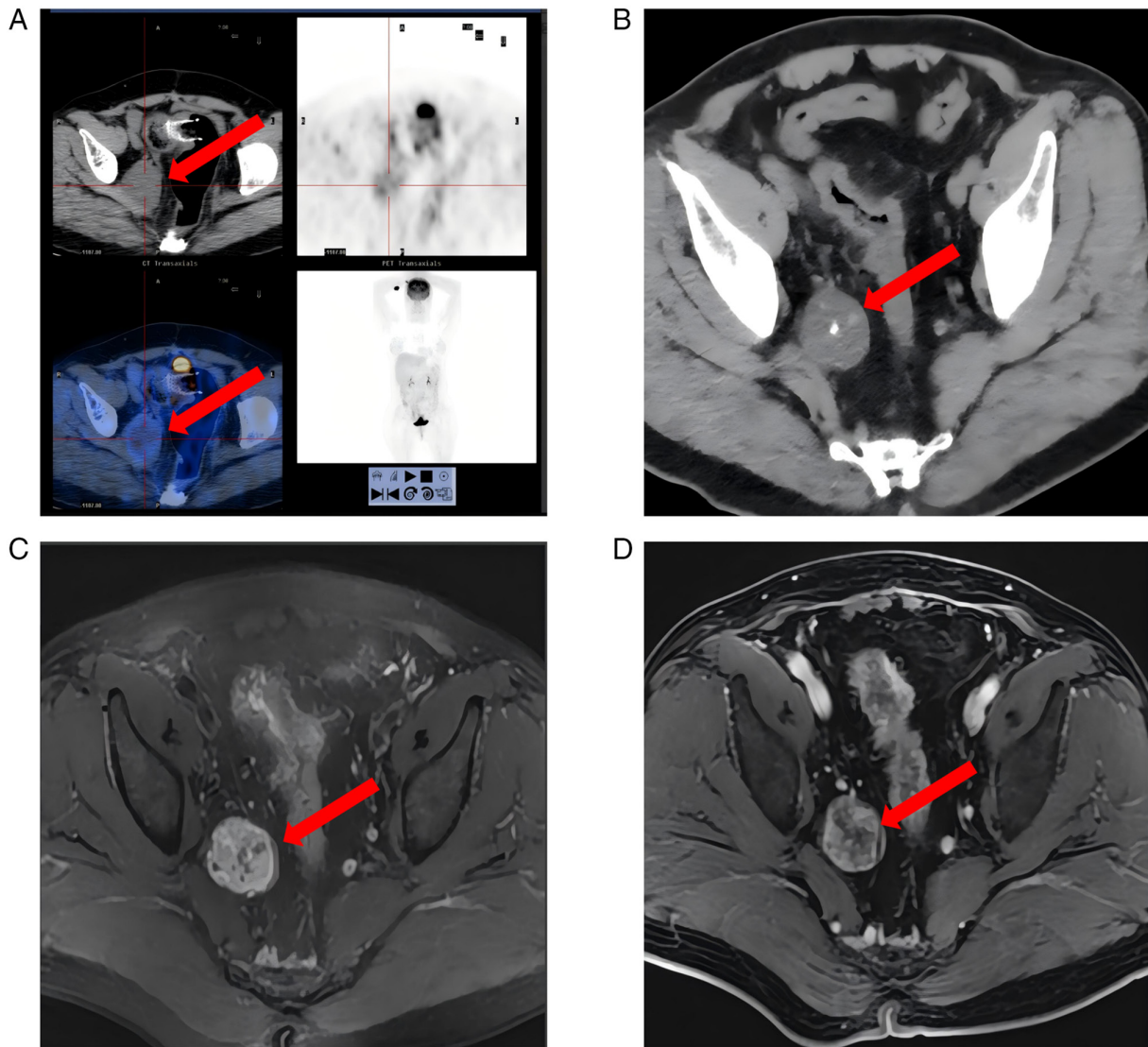


Figure 1. PET-CT images of pelvic schwannoma in case 1, and CT and MRI of pelvic schwannoma in case 2. (A) PET-CT image (case 1): A round, low-density mass (CT value, 27 HU) (red arrow) measuring 5.4x4.8 cm is evident on the right pelvic wall, exhibiting clear margins, intact perimetrium, no apparent haemorrhage, necrosis or calcification, homogeneous density, and no significant enhancement on contrast-enhanced images. PET imaging demonstrates slightly increased metabolism (SUV_{max} , 2.8). (B) Contrast-enhanced CT image (case 2): A rounded mass (red arrow) with mixed density is observed on the right pelvic wall, featuring internal calcifications and mild-to-moderate heterogeneous enhancement after contrast administration. (C) T2-weighted fat-suppressed MRI (case 2): A nodular mass (3.2x3.4 cm) (red arrow) is noted in the right pelvic obturator region, appearing slightly hyperintense with heterogeneous signal intensity. (D) Contrast-enhanced MRI (case 2): The mass (red arrow) in the right pelvic obturator region displays heterogeneous enhancement post-contrast, with scattered punctate low-signal areas observed centrally. PET-CT, positron emission tomography-computed tomography; MRI, magnetic resonance imaging; SUV_{max} , maximum standardised uptake value.

(^{18}F -FDG) positron emission tomography-computed tomography (PET-CT) findings demonstrated: i) Localised thickening at the rectosigmoid junction with slight hypermetabolism [maximum standardised uptake value (SUV_{max} , 2.8), suggestive of malignancy with possible extraserosal invasion; and ii) a soft-tissue-density mass on the medial aspect of the right pelvic wall, also with slight hypermetabolism (SUV_{max} , 2.8), raising suspicion of metastasis (Fig. 1A). After multidisciplinary team (MDT) evaluation, the patient was assigned a preliminary clinical stage of cT4NxM1 based on the National Comprehensive Cancer Network (NCCN) Clinical Practice Guidelines in Oncology for Colorectal Cancer (9,10), and subsequently received six cycles of neoadjuvant therapy at 3-week intervals. KRAS mutation testing had been performed prior to treatment using the amplification refractory mutation

system (ARMS) fluorescence quantitative PCR method on a tumor biopsy specimen obtained from the patient. However, the molecular pathology results were not yet available at the time of treatment initiation. After a thorough discussion of the potential benefits and risks with the patient and her family, it was decided to proceed with neoadjuvant therapy as scheduled. The initial regimen was FOLFOXIRI, comprising irinotecan (200 mg intravenous infusion on day 1), oxaliplatin (120 mg intravenous infusion on day 1), calcium levofolinate (300 mg intravenous infusion on day 1) and fluorouracil (3,000 mg continuous intravenous infusion over 44 h). Given the subsequently confirmed KRAS mutation, bevacizumab (300 mg intravenous infusion) was added from the second cycle onward. Due to the occurrence of Common Terminology Criteria for Adverse Events grade 2 myelosuppression (11), the regimen

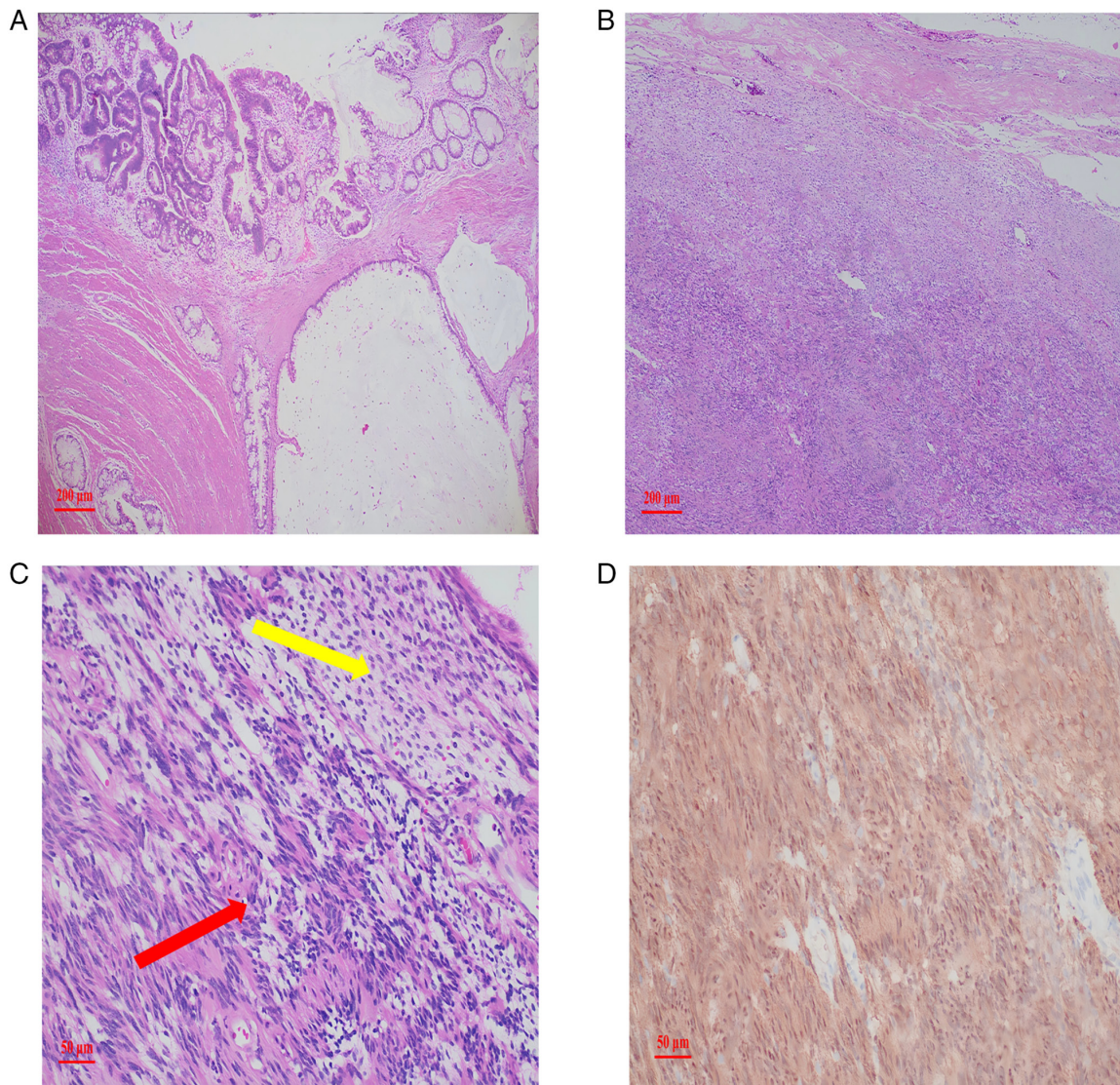


Figure 2. Microscopic views and immunohistochemical staining of pathological specimens from sigmoid colon carcinoma and pelvic schwannoma (case 1). (A) Sigmoid colon adenocarcinoma (H&E stain; x40 magnification). (B) Low-magnification view of pelvic schwannoma showing well-defined borders and encapsulation (H&E stain; x40 magnification). (C) Medium-magnification view of pelvic schwannoma: Antoni A areas (red arrow) and Antoni B areas (yellow arrow) are visible (H&E stain; x200 magnification). (D) Immunohistochemical staining of pelvic schwannoma demonstrating positive expression of S-100 protein.

was adjusted to FOLFOX (120 mg oxaliplatin intravenously on day 1, 300 mg calcium leufofolinate intravenously on day 1 and 500 mg fluorouracil by intravenous bolus followed by a continuous infusion of 3,000 mg over 44 h) for the remaining two cycles. Subsequent pelvic CT indicated regression of both the intestinal lesion and the right pelvic wall mass (Figs. S1B-D and S2). The patient then underwent radical resection of the sigmoid colon carcinoma along with excision of the mass from the right pelvic wall. Postoperative pathology confirmed moderately differentiated adenocarcinoma of the sigmoid colon (Fig. 2A) with focal residual mucinous adenocarcinoma involving the serosal membrane. Histological examination of the right pelvic wall mass revealed alternating Antoni A areas containing densely packed spindle cells and Antoni B areas with sparsely distributed spindle cells (Fig. 2B and C), and immunohistochemical staining revealed positivity for S-100 (Fig. 2D), establishing the diagnosis of a schwannoma. Immunohistochemical staining was performed on surgical

specimens using the EliVision two-step method. Briefly, 3- μ m thick paraffin sections were dewaxed and rehydrated, followed by blocking endogenous peroxidase activity with 3% hydrogen peroxide (H₂O₂) at room temperature for 10 min. Sections were incubated with a ready-to-use primary antibody against S-100 protein [cat. no. B26011908; Hangzhou Bailing (Biolynx) Biotechnology Co., Ltd.] at 28°C for 40 min, washed, and subsequently incubated with a ready-to-use horseradish peroxidase (HRP)-conjugated EnVision secondary antibody (cat. no. 2603020805B; Fuzhou Maixin Biotechnology Development Co., Ltd.) at 28°C for 40 min. Immunoreactivity was visualized with 3,3'-diaminobenzidine chromogen at 28°C for 15 min, followed by hematoxylin counterstaining. Slides were observed under an OLYMPUS BX53 light microscope.

Following the operation, the patient underwent postoperative adjuvant therapy at the 900th Hospital of PLA Joint Logistic Support Force. Initially, two cycles of the CAPEOX regimen were administered, comprising intravenous

Table I. Differential diagnosis between pelvic schwannomas and pelvic metastases originating from colorectal cancer.

Feature	Pelvic schwannoma	Pelvic metastasis from colorectal cancer	(Refs.)
Growth pattern	Slow, expansive growth with clear margins and encapsulation	Rapid, invasive growth with indistinct boundaries, infiltrating surrounding tissues	(4,56)
Relationship with nerves and blood vessels	Arises from the nerve sheath (sacral/hypogastric plexus), showing the 'entering and exiting nerve sign', and displaces vessels without invasion.	No direct neural involvement initially; advanced stages may involve the sacral plexus. EMVI is common, with vessels encircling the lesion and lymph node metastasis.	(57-59)
Imaging findings	CT: A well-defined hypodense mass on non-contrast CT, with either homogeneous or heterogeneous attenuation. MRI: Hypointense on T1WI and hyperintense on T2WI, with hallmark features including the 'target sign', 'entering and exiting nerve sign' and 'fat-splitting sign' observed in a subset of cases. PET-CT: Highly variable metabolic activity, with a mean SUV _{max} of 5.4±2.7.	CT: A soft-tissue mass with indistinct boundaries, heterogeneous density and uneven enhancement. MRI: Hypointense on T1WI, isointense on T2WI and hyperintense on DWI. PET-CT: Demonstrates significant hypermetabolic activity.	(19,22,43,60,61)

EMVI, extramural vascular invasion; PET-CT, positron emission tomography-computed tomography; MRI, magnetic resonance imaging; WI, weighted imaging; DWI, diffusion WI; SUV_{max}, maximum standardised uptake value.

oxaliplatin (180 mg) on day 1, and oral capecitabine at doses of 1,000 mg in the morning and 1,500 mg in the evening on days 1-14, repeated every 3 weeks. Subsequently, imaging follow-up suggested possible tumour recurrence and metastasis. Therefore, the treatment was revised to a 3-week cycle regimen consisting of oral capecitabine (1.5 g twice daily, days 1-14), trifluridine-tipiracil (TAS102; 50 mg orally twice daily, days 1-5) and bevacizumab (300 mg). All three agents were administered on a 3-week cycle. To date, the patient has completed five cycles of this revised regimen. Regular post-operative follow-up has been conducted every 3 weeks, and at the most recent evaluation, the patient remained in stable condition.

ARMS fluorescence quantitative PCR. Genomic DNA was isolated from 10- μ m thick formalin-fixed, paraffin-embedded (FFPE) tumor tissue sections using the Nucleic Acid Extraction Kit (FFPE DNA; Amoy Diagnostics Co., Ltd.) according to the manufacturer's instructions, and only samples with a concentration >2 ng/ μ l and with an OD₂₆₀/OD₂₈₀ ratio between 1.8 and 2.0 as measured by a Nanodrop 2000 spectrophotometer (Thermo Fisher Scientific, Inc.) were used for subsequent analysis. Detection of KRAS, NRAS, PIK3CA and BRAF mutations was performed with the Human KRAS/NRAS/PIK3CA/BRAF Gene Mutation Joint Detection

Kit (fluorescence PCR; cat. no. 801.0173; Amoy Diagnostics Co., Ltd.), which is based on the amplification refractory mutation system ARMS fluorescent quantitative PCR. The reaction mixture was prepared by combining 65.8 μ l of extracted DNA with 4.2 μ l of the supplied KNPB Enzyme Mix, which contained a thermostable DNA polymerase, specific forward and reverse primers, fluorescent probes and internal control components; the sequences of the forward and reverse primers are proprietary to the kit and were not disclosed by the manufacturer. After brief vortexing and centrifugation, 5 μ l of the mixture was dispensed into each tube of the 12-strip PCR array. Amplification and fluorescence detection were carried out on an ABI 7500 Real-Time PCR System with the following dye settings: Reporter dye, FAM and VIC; quencher dye, TAMRA; passive reference, nONE. Thermal cycling conditions were as follows: Initial denaturation at 95°C for 5 min (1 cycle); followed by 15 cycles of denaturation at 95°C for 25 sec, annealing at 64°C for 20 sec and extension at 72°C for 20 sec; then 31 cycles of denaturation at 93°C for 25 sec, annealing at 60°C for 35 sec (fluorescence signal acquisition during this step) and extension at 72°C for 20 sec. No agarose gel electrophoresis was performed, as the assay directly monitors amplicon accumulation via real-time fluorescence. Mutation status was assigned according to the manufacturer's cut-off criteria: A FAM Cq value \leq 26 in a mutation-specific

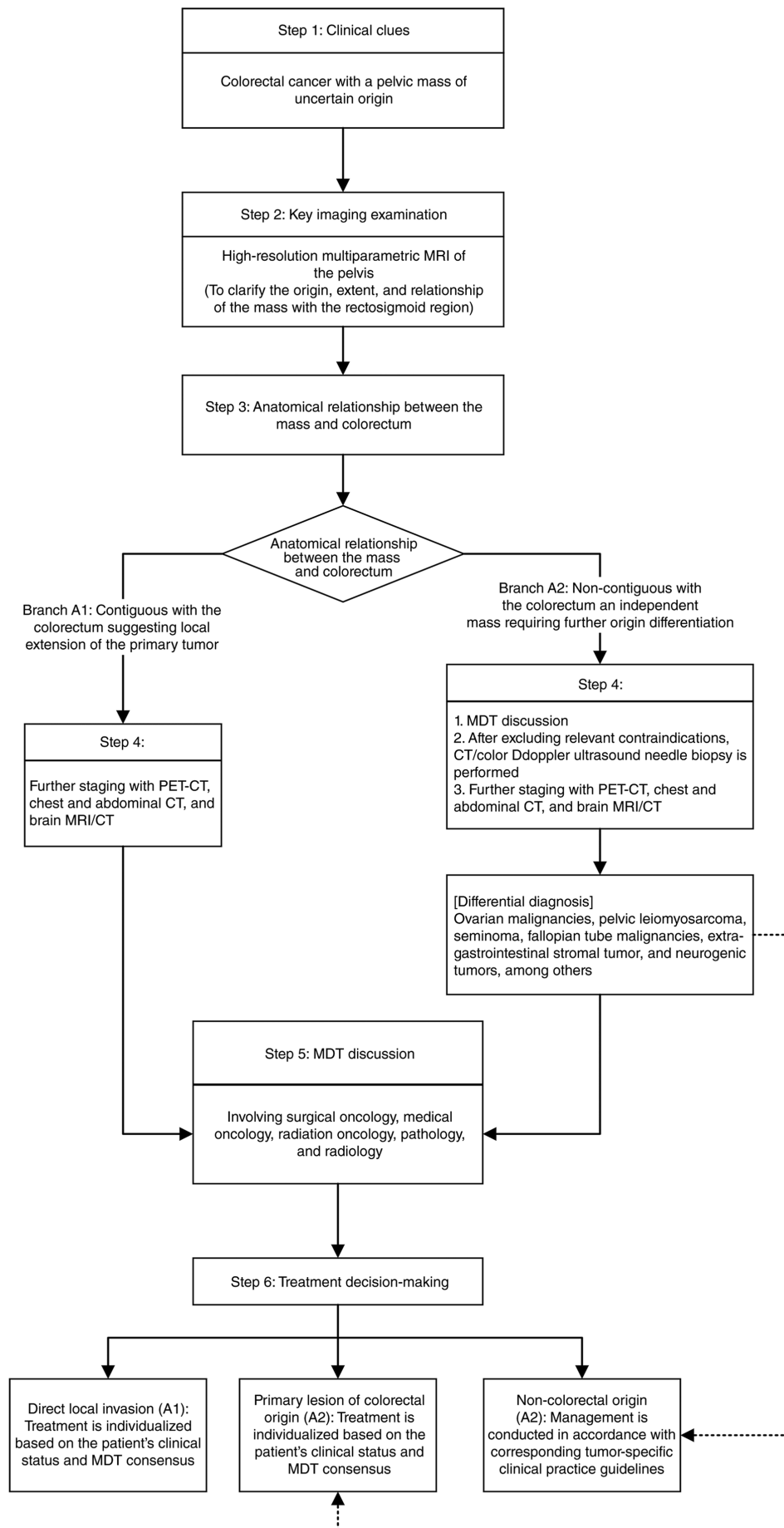


Figure 3. Diagnostic flowchart for evaluating patients with colorectal cancer presenting with pelvic masses of uncertain origin. MDT, multidisciplinary team; PET-CT, positron emission tomography-computed tomography; MRI, magnetic resonance imaging.

reaction tube, with a valid VIC (internal control) signal, was considered positive for the corresponding mutation; a FAM Cq value >26 or undetermined was considered negative. The positive control was required to yield Cq values <20 for both FAM and VIC, and the no-template control had to be free of FAM amplification.

Case 2. A 73-year-old man was admitted to the 900th Hospital of PLA Joint Logistic Support Force with an 8-year history of intermittent haematochezia. Colonoscopy revealed an irregular mass located 15-19 cm from the anal verge, occupying approximately one-half of the intestinal lumen, with surface erosion and necrosis; biopsy pathology suggested moderately differentiated adenocarcinoma (Fig. S3A). Pelvic CT findings indicated: i) Sigmoid colon cancer with metastasis to the regional mesenteric lymph nodes; and ii) a mass with calcification adjacent to the iliac vessels in the right pelvic wall peritoneal region, suggestive of a tumour, with metastatic disease not excluded (Fig. 1B). Pelvic magnetic resonance imaging (MRI) demonstrated: i) Sigmoid colon cancer with regional mesenteric lymph node metastasis; and ii) a mass on the right pelvic wall, with metastasis considered likely (Fig. 1C and D). MDT discussion determined the clinical stage to be T₃N₊M₁ based on the NCCN Clinical Practice Guidelines in Oncology for Colorectal Cancer (9,10). The patient underwent six cycles of neoadjuvant therapy consisting of the CAPEOX regimen combined with bevacizumab, administered every 3 weeks for a total of 18 weeks. The specific regimen included oxaliplatin (200 mg intravenous infusion on day 1), oral capecitabine at doses of 1,000 mg in the morning and 1,500 mg in the evening on days 1-14 and bevacizumab (300-400 mg intravenous infusion on day 1). After six cycles of neoadjuvant therapy, follow-up evaluation showed that the colonic lesion had decreased in size, whereas the right pelvic wall mass remained largely unchanged (Figs. S4 and S5). Subsequently, the patient underwent a radical resection of sigmoid colon cancer and an excision of the right pelvic wall mass. Postoperative pathology confirmed the initial diagnosis of moderately differentiated adenocarcinoma of the sigmoid colon (Fig. S3B); following neoadjuvant therapy, only scattered residual tumour nests were identified after extensive sampling. Histopathological examination of the right pelvic wall mass again revealed alternating Antoni A and B areas, with immunohistochemical positivity for S-100, confirming a schwannoma (Fig. S3C and D). No adjuvant therapy was administered postoperatively. Monthly telephone follow-ups indicated stable clinical status, and regular clinical evaluations were performed at a local hospital.

Discussion

According to the latest 2022 GLOBOCAN estimates from the International Agency for Research on Cancer, the global burden of colorectal cancer has increased significantly over the past decade, with absolute increases in new cases and deaths of 41.5 and 34.7%, respectively (12,13). Previous studies (14,15) have indicated that $>20\%$ of patients with colorectal cancer present with distant metastases to sites such as the liver, lung, peritoneum and ovary at the initial diagnosis. Approximately one-quarter of patients exhibit peritoneal metastases, and

these patients typically have a poor prognosis. Furthermore, colorectal cancer represents a common primary origin for ovarian metastases (16,17).

Schwannomas originate from well-differentiated Schwann cells, and the vast majority of these tumours are benign (1). Malignant schwannomas are rare and are often associated with neurofibromatosis (18). Pelvic schwannomas are uncommon clinically, and some researchers (3) have proposed that they originate from the peripheral nerve sheath of the sacral nerve or the hypogastric plexus. A solitary, intact and well-defined capsule is characteristic of schwannomas; however, pelvic schwannomas often demonstrate atypical presentations, including cystic degeneration, haemorrhage and calcification (3,8). Due to their slow growth and non-specific clinical symptoms, pelvic schwannomas are challenging to detect at an early stage; they typically become noticeable only when compression or invasion of adjacent tissues and organs causes corresponding symptoms (2). Imaging studies indicate that pelvic schwannomas frequently appear as well-defined, hypodense lesions on CT scans (19). Compared with CT, MRI offers superior visualisation of pelvic masses, demonstrating higher sensitivity and specificity for detecting schwannomas (20,21). Clinical studies (22,23) have shown schwannomas to typically exhibit hypointensity on T1-weighted imaging (T1WI), hyperintensity on T2WI, and heterogeneous enhancement following contrast administration on T1WI; these features are consistent with the MRI findings observed in the cases of the present study. Notably, scholarly opinions differ on the diagnostic certainty achievable by preoperative imaging alone. Tong *et al* (24) suggested that confirmation of the association between the pelvic mass and peripheral nerves or blood vessels through imaging is critical for diagnosing schwannomas. By contrast, Wu *et al* (7) concluded that imaging of pelvic schwannomas lacks specificity, making differentiation from other pelvic masses difficult. In pathological assessments, apart from the specific immunohistochemical marker S-100, positive staining for neuron-specific enolase and microfilament proteins has also been reported to support the diagnosis of schwannomas (25-27). Microscopically, schwannomas are composed of densely packed spindle-shaped cells (Antoni A areas) and loosely arranged tumour cells (Antoni B areas) (8,28). Currently, surgical resection is the optimal treatment for schwannomas (7). An intercontinental multicenter study (29) recommended MDT discussions before pelvic schwannoma resection to determine whether local or radical resection is appropriate, considering both the patient's postoperative prognosis and the anatomical relationships with surrounding nerves and blood vessels. Damage to pelvic peripheral nerves and vessels during surgery may lead to neurological impairment (8,30). In the follow-up described for case 1, the patient presented with localized postoperative neurological dysfunction, manifested as numbness, pain and cold sensory paresthesia in the right lower extremity. Consequently, preoperative MDT evaluation is particularly important in managing pelvic schwannomas.

Common to both cases reported in the present study was the preoperative misdiagnosis of a pelvic schwannoma as a metastatic lesion originating from colorectal cancer. The reasons are as follows: First, schwannomas typically occur in the head, neck and limbs, with pelvic schwannomas being

rare (31). Second, symptoms associated with pelvic schwannomas lack specificity and vary according to the lesion's size and location (27). The absence of specific clinical manifestations in both cases described within the present study further complicated the preoperative diagnosis. Third, imaging findings in pelvic schwannomas, which often exhibit rich blood supply and atypical features such as cystic degeneration, liquefaction necrosis and calcification, are easily mistaken for malignant pelvic tumours without histopathological confirmation (3,32,33). Malignant ovarian tumours commonly present as mixed cystic-solid, solid or cystic masses on CT scans, and MRI may reveal cystic-solid lesions or nodular structures similar to schwannomas, with high signal intensity on diffusion-weighted imaging (DWI) and heterogeneous enhancement following contrast administration (34-36). Pelvic malignancies, including leiomyosarcoma, seminoma, fallopian tube carcinoma and extra-gastrointestinal stromal tumours, also share imaging characteristics with schwannomas (37-42). Advanced MRI techniques, including contrast-enhanced magnetic resonance neurography (CE-MRN) and DWI, offer distinct advantages over conventional MRI in identifying neurogenic tumours in the pelvic region (43-45). However, CE-MRN exhibits lower spatial resolution compared with conventional MRI, limiting its ability to adequately evaluate tumour microstructure, function or metabolism (43). In addition, schwannomas frequently present with cystic degeneration and necrosis, leading to pseudo-limited diffusion on DWI (46). Therefore, these techniques should be combined with other imaging modalities for more accurate assessment. Additionally, ^{18}F -FDG is a non-specific tracer that can exhibit increased uptake not only in malignant tumours but also in some benign lesions, leading to false-positive results (47-49). In case 1 of the present study, preoperative ^{18}F -FDG PET-CT also demonstrated mild hypermetabolism. Boré *et al* (49) argued that false-positive ^{18}F -FDG findings could influence preoperative diagnosis and treatment decisions in patients with schwannomas. Currently, pathological examination following complete surgical resection remains the gold standard for diagnosing schwannomas.

Upon reviewing the imaging data of the two pelvic mass cases presented within the current study, although no characteristic imaging features were identified, both lesions were located in anatomical regions along the pelvic wall or obturator nerve plexus, suggesting the possibility of schwannomas. In addition, when a pelvic mass demonstrates imaging features such as the target sign and nerve entry-exit sign with well-defined margins, schwannoma should also be included in the routine differential diagnosis (43). A previous report has described a case in which a peritoneal mass was misdiagnosed as a metastatic malignant lesion. Similar to cases 1 and 2 in the present report, after MDT discussion, no preoperative biopsy was performed, and the diagnosis of schwannoma was ultimately confirmed by postoperative pathological examination (50). This has prompted consideration of how the MDT model could be further improved in preoperative diagnostic decision-making. Preoperative biopsy is necessary; however, preoperative biopsy of schwannomas is prone to sampling error due to tumour cell degeneration and pleomorphism, which may lead to misdiagnosis (51). Therefore, the involvement of subspecialty radiologists (such as musculoskeletal or pelvic radiologists) in multidisciplinary diagnosis and treatment processes for pelvic masses is essential

for providing specialised imaging consultations. Additionally, greater emphasis should be placed on comparing imaging morphology, lesion invasion extent and preoperative biopsy histopathological characteristics during MDT discussions to improve the accuracy of preoperative assessments (52,53). Although pelvic schwannomas have previously been misdiagnosed as malignant tumours (54,55), most existing studies have not systematically summarised the key points for differentiating pelvic schwannomas from pelvic metastatic lesions of colorectal cancer. Furthermore, no standardised clinical diagnosis and treatment protocol has been established for patients with colorectal cancer complicated by pelvic masses. Based on the diagnostic experience from the present cases, we believe it is clinically valuable to establish a clear, practical and systematic diagnostic pathway and optimise MDT evaluations for patients with colorectal cancer presenting with pelvic masses. Based on prior literature, the present study analysed the distinguishing features between pelvic schwannomas and colorectal cancer pelvic metastatic lesions in terms of growth patterns, associations with neurovascular structures and imaging characteristics (Table I) (4,19,22,43,56-61). Pelvic schwannomas typically exhibit slow growth with clear margins, originate from the nerve sheath (sacral or hypogastric plexus), demonstrate the 'entering and exiting nerve sign' and lack vascular invasion. Radiologically, schwannomas appear as well-defined hypodense masses on non-contrast CT, demonstrate T1-hypointensity and T2-hyperintensity on MRI (occasionally exhibiting the 'target sign' or 'fat-splitting sign'), and show variable metabolic activity on PET-CT. By contrast, colorectal cancer pelvic metastases grow rapidly and invasively with indistinct boundaries, initially lack direct neural involvement (with potential sacral plexus involvement at advanced stages), and EMVI, vascular encirclement and lymph node metastasis. Imaging typically reveals ill-defined soft-tissue masses with heterogeneous density and uneven enhancement on CT, T1-hypointensity, T2-isointensity and DWI hyperintensity on MRI, along with markedly hypermetabolic activity on PET-CT (4,19,22,43,56-61). In addition, we propose a standardised diagnostic and therapeutic workflow for patients with colorectal cancer and pelvic masses of unknown origin (Fig. 3), aiming to provide guidance and reference for clinical decision-making in similar cases. This workflow initiates with clinical screening of patients with who present with pelvic masses of uncertain etiology. High-resolution multiparametric pelvic MRI is employed to clarify lesion origin, invasive extent, and anatomical relationships between pelvic lesions and the rectosigmoid colon. Patients are then stratified into two treatment pathways based on the spatial continuity between lesions and the intestinal tract: Masses adjacent to the bowel indicate local infiltration by primary colorectal cancer, necessitating systematic examinations for accurate tumour staging. For isolated pelvic lesions unrelated to the colorectum, preliminary MDT consultation should occur first, followed by image-guided needle biopsy after excluding contraindications, combined with whole-body staging assessments and differential diagnosis of common pelvic tumours. A subsequent multidisciplinary consensus discussion is then held to formulate personalized therapeutic regimens.

In conclusion, the current study presents two cases of pelvic schwannomas initially misdiagnosed as colorectal cancer metastases. This misdiagnosis underscores the

importance of preoperative differential diagnosis in evaluating pelvic masses. Additionally, the diagnostic challenge is further complicated by the non-specific clinical and imaging features of pelvic schwannomas. Postoperative pathological examination remains essential for a definitive diagnosis. The present case report and associated retrospective analysis highlight the necessity for clinicians to consider pelvic schwannomas when investigating the origin of pelvic masses.

Acknowledgements

Not applicable.

Funding

No funding was received.

Availability of data and materials

The data generated in the present study may be requested from the corresponding author.

Authors' contributions

SW made substantial contributions to the conception and design of the study, acquisition, organization and analysis of clinical data, as well as drafting the initial manuscript. JL participated in the critical revision of the manuscript for important intellectual content, provided academic guidance on the study design and data interpretation, and gave final approval of the version to be published. KZ and XL were involved in the identification of study cases, acquisition and preliminary analysis of clinical data, coordination of patient follow-up, and participated in the discussion of individual patient treatment plans. FX and JY made substantial contributions to the acquisition, analysis and professional interpretation of imaging data and pathological specimen images, provided key imaging and pathological evidence for the diagnosis and treatment of cases, and participated in the revision of the manuscript related to imaging and pathology. All authors have made substantial intellectual contributions to the study. All authors read and approved the final manuscript, and agreed to be accountable for all aspects of the work to ensure that any questions related to the accuracy or integrity of the work are appropriately investigated and resolved. SW and JL confirm the authenticity of all the raw data.

Ethics approval and consent to participate

Not applicable.

Patient consent for publication

Written informed consent was obtained from the patients for the publication of their clinical data and accompanying images.

Competing interests

The authors declare that they have no competing interests.

References

- Lee SH, Lee SJ and Lee CS: A rare case of pelvic concurrent schwannoma(neurilemmoma) and neurofibroma. *Asian J Surg* 45: 1084-1085, 2022.
- Bulut AL, Nyangoh Timoh K, Bretonnier M, Lavoué V, Morandi X and Levêque J: Case report: Dyspareunia as a symptom of a pelvic schwannoma. *J Gynecol Obstet Hum Reprod* 51: 102402, 2022.
- Dau MHT, Tran MTT, Nguyen HQ, Vo KYT, Nguyen TTT, Hoang TH, Hoang VT and Hoang DT: Pelvic schwannoma in an adult male. *Acta Radiol Open* 11: 20584601221102822, 2022.
- Kawahori T, Mukai S, Saito Y, Nishida T, Fukuda T and Ohdan H: A rare case of giant pelvic retroperitoneal schwannoma. *Radiol Case Rep* 19: 5738-5743, 2024.
- Santos AJ, Duarte L, Santos SC and Casimiro C: A 68-year-old woman presenting with recurrent abdominal pain and a diagnosis of a presacral retroperitoneal benign schwannoma that mimicked an ovarian tumor on pelvic magnetic resonance imaging. *Am J Case Rep* 23: e935985, 2022.
- Kalagi D, Bakir M, Alfarra M, Aborayya A and Anwar I: Two unusual presentations of presacral schwannoma; a case series. *Int J Surg Case Rep* 61: 165-168, 2019.
- Wu X, Meng H, Fan Q, Qi Z and Pan W: Image features and clinical analysis of retroperitoneal pelvic schwannoma: A case report. *BMC Neurol* 24: 230, 2024.
- Zhou S, Wan S, Li L, Dong W, Ma X, Chu H and Zhong Y: Rare retroperitoneal giant sacral schwannoma: A case report. *Oncol Lett* 27: 261, 2024.
- Benson AB, Venook AP, Adam M, Chang G, Chen YJ, Ciombor KK, Cohen SA, Cooper HS, Deming D, Garrido-Laguna I, *et al*: Colon cancer, version 3.2024, NCCN clinical practice guidelines in oncology. *J Natl Compr Canc Netw* 22: e240029, 2024.
- Amin MB, Edge SB, Greene FL, Byrd DR, Brookland RK, Washington MK, Gershenwald JE, Compton CC, Hess KR, Sullivan DC, *et al*: AJCC cancer staging manual. 8th ed. Springer International Publishing, Cham, 2017.
- National Cancer Institute: Common Terminology Criteria for Adverse Events (CTCAE) Version 5.0. National Institutes of Health, Bethesda, MD, 2017.
- No authors listed: Global cancer burden growing, amidst mounting need for services. *Saudi Med J* 45: 326-327, 2024.
- Bray F, Laversanne M, Sung H, Ferlay J, Siegel RL, Soerjomataram I and Jemal A: Global cancer statistics 2022: GLOBOCAN estimates of incidence and mortality worldwide for 36 cancers in 185 countries. *CA Cancer J Clin* 74: 229-263, 2024.
- He K, Wang Z, Luo M, Li B, Ding N, Li L, He B, Wang H, Cao J, Huang C, *et al*: Metastasis organotropism in colorectal cancer: Advancing toward innovative therapies. *J Transl Med* 21: 612, 2023.
- Vatandoust S, Price TJ and Karapetis CS: Colorectal cancer: Metastases to a single organ. *World J Gastroenterol* 21: 11767-11776, 2015.
- Franko J, Shi Q, Meyers JP, Maughan TS, Adams RA, Seymour MT, Saltz L, Punt CJA, Koopman M, Tournigand C, *et al*: Prognosis of patients with peritoneal metastatic colorectal cancer given systemic therapy: An analysis of individual patient data from prospective randomised trials from the analysis and research in cancers of the digestive system (ARCAD) database. *Lancet Oncol* 17: 1709-1719, 2016.
- Franko J, Shi Q, Goldman CD, Pockaj BA, Nelson GD, Goldberg RM, Pitot HC, Grothey A, Alberts SR and Sargent DJ: Treatment of colorectal peritoneal carcinomatosis with systemic chemotherapy: A pooled analysis of north central cancer treatment group phase III trials N9741 and N9841. *J Clin Oncol* 30: 263-267, 2012.
- Yao C, Zhou H, Dong Y, Alhaskawi A, Hasan Abdullah Ezzi S, Wang Z, Lai J, Goutham Kota V, Hasan Abdulla Hasan Abdulla M and Lu H: Malignant peripheral nerve sheath tumors: Latest concepts in disease pathogenesis and clinical management. *Cancers (Basel)* 15: 1077, 2023.
- Nasu K, Arima K, Yoshimatsu J and Miyakawa I: CT and MRI findings in a case of pelvic schwannoma. *Gynecol Obstet Invest* 46: 142-144, 1998.
- Elsherif SB, Agely A, Gopireddy DR, Ganeshan D, Hew KE, Sharma S and Lall C: Mimics and pitfalls of primary ovarian malignancy imaging. *Tomography* 8: 100-119, 2022.

21. Schraepen C, Donkersloot P, Duyvendak W, Plazier M, Put E, Roosen G, Vanvolsem S, Wissels M and Bamps S: What to know about schwannomatosis: A literature review. *Br J Neurosurg* 36: 171-174, 2022.
22. Conde Vasco I, Martins Pereira G, Ferreira J and Cunha TM: Schwannoma mimicking ovarian malignancy. *Radiol Case Rep* 17: 4308-4313, 2022.
23. Crist J, Hodge JR, Frick M, Leung FP, Hsu E, Gi MT and Venkatesh SK: Magnetic resonance imaging appearance of schwannomas from head to toe: A pictorial review. *J Clin Imaging Sci* 7: 38, 2017.
24. Tong RSK, Collier N and Kaye AH: Chronic sciatica secondary to retroperitoneal pelvic schwannoma. *J Clin Neurosci* 10: 108-111, 2003.
25. Zareharifi N, Karimzadgh S, Ebrahimian R, Reihanian Z, Abbaspour E, Karimian P and Taheri Talesh J: Successful management of a giant retroperitoneal ancient schwannoma mimicking malignant tumors: A case report and literature review. *Ann Med Surg (Lond)* 85: 6279-6284, 2023.
26. Chen W, Dang C, Zhu K and Li K: Preoperative management of giant retroperitoneal schwannoma: A case report and review of the literature. *Oncol Lett* 11: 4030-4034, 2016.
27. Machairiotis N, Zarogoulidis P, Stylianaki A, Karatrasoglou E, Sotiropoulou G, Floreskou A, Chatzi E, Karamani A, Liapi G, Papakonstantinou E, *et al*: Pelvic schwannoma in the right parametrium. *Int J Gen Med* 6: 123-126, 2013.
28. Leclerc A, Lebreton G, Huet A, Alves A and Emery E: Management of giant presacral schwannoma. Clinical series and literature review. *Clin Neurol Neurosurg* 200: 106409, 2021.
29. Transatlantic Australasian Retroperitoneal Sarcoma Working Group: Intercontinental collaborative experience with abdominal, retroperitoneal and pelvic schwannomas. *Br J Surg* 107: 452-463, 2020.
30. Cho DH: Retroperitoneal schwannoma misdiagnosed as an ovarian malignancy. *BMJ Case Rep* 2018: bcr2018225502, 2018.
31. Attia H, Agboola JO, Seong G, Thida A, Chiu E and Agaronov M: Synchronous pelvic schwannoma with metastatic prostate cancer: A rare case and pathology review. *Cureus* 16: e52356, 2024.
32. Hughes MJ, Thomas JM, Fisher C and Moskovic EC: Imaging features of retroperitoneal and pelvic schwannomas. *Clin Radiol* 60: 886-893, 2005.
33. Jindal T, Mukherjee S, Kamal MR, Sharma RK, Ghosh N, Mandal SN, Das AK and Karmakar D: Cystic schwannoma of the pelvis. *Ann R Coll Surg Engl* 95: e1-e2, 2013.
34. Bourgioti C, Konidari M and Mouloupoulos LA: Manifestations of ovarian cancer in relation to other pelvic diseases by MRI. *Cancers (Basel)* 15: 2106, 2023.
35. Chen Z, Liu Z, Yang J, Sun J and Wang P: The clinicopathological characteristics, prognosis, and CT features of ovary metastasis from colorectal carcinoma. *Transl Cancer Res* 10: 3248-3258, 2021.
36. Foti PV, Attinà G, Spadola S, Caltabiano R, Farina R, Palmucci S, Zarbo G, Zarbo R, D'Arrigo M, Milone P and Ettore GC: MR imaging of ovarian masses: Classification and differential diagnosis. *Insights Imaging* 7: 21-41, 2016.
37. Marko J and Wolfman DJ: Retroperitoneal leiomyosarcoma from the radiologic pathology archives. *Radiographics* 38: 1403-1420, 2018.
38. Marko J, Wolfman DJ, Aubin AL and Sesterhenn IA: Testicular seminoma and its mimics: From the radiologic pathology archives. *Radiographics* 37: 1085-1098, 2017.
39. Veloso Gomes F, Dias JL, Lucas R and Cunha TM: Primary fallopian tube carcinoma: Review of MR imaging findings. *Insights Imaging* 6: 431-439, 2015.
40. Dande A, Pajai S, Acharya N, Joshi KS, Patel DJ and Gupta A: Gastrointestinal stromal tumors mimicking ovarian mass: A case report. *Cureus* 16: e58320, 2024.
41. Arellano-Gutiérrez G, Martínez-Aldrete LF, Pérez-Fabián A and Maldonado-García EL: Primary extra-gastrointestinal stromal tumor (EGIST) of the mesentery: Case report and review of literature. *Ann Med Surg (Lond)* 60: 480-483, 2020.
42. Watal P, Brahmabhatt SG, Thoriya PJ and Bahri NU: Retroperitoneal extragastrointestinal stromal tumor: Radiologic pathologic correlation. *J Clin Imaging Sci* 4: 34, 2014.
43. Wu W, Ding Y, Su Y, Wang Y, Liu T, Zhang Z, Liu D, Li C, Zheng C and Wang L: Novel MRI signs for differentiating neurogenic and non-neurogenic peripheral nerve tumors: Insights from contrast-enhanced magnetic resonance neurography. *Eur J Radiol* 183: 111894, 2025.
44. Ristow I, Apostolova I, Kaul MG, Stark M, Zapf A, Schmalhofer ML, Mautner VF, Farschtschi S, Adam G, Bannas P, *et al*: Discrimination of benign, atypical, and malignant peripheral nerve sheath tumours in neurofibromatosis type 1-intra-individual comparison of positron emission computed tomography and diffusion-weighted magnetic resonance imaging. *EJNMMI Res* 14: 127, 2024.
45. Yuh EL, Jain Palrecha S, Lagemann GM, Kliot M, Weinstein PR, Barbaro NM and Chin CT: Diffusivity measurements differentiate benign from malignant lesions in patients with peripheral neuropathy or plexopathy. *AJNR Am J Neuroradiol* 36: 202-209, 2015.
46. Said EN, Mohamed DHE, Abdellatif RS, Nashed GA and Beshir MMR: Radiological pitfalls in DWI in characterization of primary retroperitoneal masses. *Med. J. Cairo Univ* 91: 245-257, 2023.
47. Long NM and Smith CS: Causes and imaging features of false positives and false negatives on F-PET/CT in oncologic imaging. *Insights Imaging* 2: 679-698, 2011.
48. Zhu Y, Wu J, Wang Y, Geng J and Zhang C: Presacral benign schwannoma mimics malignancy on 18F-FDG and 68Ga-FAPI PET/CT. *Clin Nucl Med* 47: 277-278, 2022.
49. Boré P, Descourt R, Ollivier L, Le Roux PY and Abgral R: False positive 18F-FDG positron emission tomography findings in schwannoma-A caution for reporting physicians. *Front Med (Lausanne)* 5: 275, 2018.
50. Pan S, Wang P, Chen Z, Liu Y and Zhou Z: Retroperitoneal schwannoma mimicking a metastatic lymph node of renal clear cell carcinoma: A case report. *Front Neurol* 15: 1450217, 2024.
51. Maidarti M, Wibawa YS, Garinasi PD, Hellyanti T, Harzif AK and Nuryanto KH: Rare case of pelvic schwannoma mimicking intra-ligamentary uterine fibroid: A case report. *Int J Surg Case Rep* 96: 107327, 2022.
52. Jeon SK, Kim SH, Shin CI, Yoo J, Park KJ, Ryoo SB, Park JW, Kim TY, Han SW, Lee DW, *et al*: Role of dedicated subspecialized radiologists in multidisciplinary team discussions on lower gastrointestinal tract cancers. *Korean J Radiol* 23: 732-741, 2022.
53. Beaman FD, Kransdorf MJ and Menke DM: Schwannoma: Radiologic-pathologic correlation. *Radiographics* 24: 1477-1481, 2004.
54. Chou D, Zahid A and Cheng E: Lateral pelvic wall schwannoma: A case report and literature review. *Cureus* 17: e99569, 2025.
55. Bai J, Kleysler-Sugrue K, Nerenstone SR and Welch JP: Synchronous colonic adenocarcinoma and pelvic schwannoma. *Conn Med* 75: 93-95, 2011.
56. El Asmar A, Demetter P, Fares F, Sclafani F, Hendlisz A, Donckier V, Vermeulen P and Liberale G: The prognostic value of distinct histological growth patterns of colorectal peritoneal metastases: A pilot study. *Ann Surg Oncol* 30: 3320-3328, 2023.
57. Mazzola CR, Power N, Bilsky MH, Robert R and Guillonneau B: Pudendal schwannoma: A case report and literature review. *Can Urol Assoc J* 8: E199-E203, 2014.
58. Richart V, Castillo-Fortuño A and Garcia-Diez AI: Advance imaging with magnetic resonance neurography for the diagnosis of unusual extensive pelvic perineural spread in colorectal cancer: A case report. *J Med Case Rep* 19: 191, 2025.
59. Chandramohan A, Mittal R, Dsouza R, Yezzaji H, Eapen A, Simon B, John R, Singh A, Ram TS, Jesudason MR, *et al*: Prognostic significance of MR identified EMVI, tumour deposits, mesorectal nodes and pelvic side wall disease in locally advanced rectal cancer. *Colorectal Dis* 24: 428-438, 2022.
60. Dewey BJ, Howe BM, Spinner RJ, Johnson GB, Nathan MA, Wenger DE and Broski SM: FDG PET/CT and MRI features of pathologically proven schwannomas. *Clin Nucl Med* 46: 289-296, 2021.
61. Cervantes A, Adam R, Roselló S, Arnold D, Normanno N, Taïeb J, Seligmann J, De Baere T, Osterlund P, Yoshino T, *et al*: Metastatic colorectal cancer: ESMO clinical practice guideline for diagnosis, treatment and follow-up. *Ann Oncol* 34: 10-32, 2023.

